Interactive and Wearable MIP Recognition Technique Combine Pattern recognition and Spatial Tracking based on SPG Sampling

Zhen GAN, BinBin FU, MingChui DONG
Electrical and Computer Engineering
University of Macau
Macau SAR, China
wenyayue@gmail.com ariespleo51@gmail.com dmc@sftw.umac.mo

Abstract: - Health monitoring based on sphygmogram (SPG) intelligent analysis is a promising alternative for cardiovascular diseases pre-diagnosis. Unfortunately for a wearable SPG intelligent analyzer the qualified SPG sampling is a stern challenge due to user wrist's any movement or incorrect posture (MIP) might result in distorted SPG morphology and analysis failure. Hence, using micro inertial measurement unit (MIMU) and pattern recognition technology in our previous research could solve the problem generally [3]. However, on account of the limitation of MIP database, a more powerful method on the base of MIP pattern recognition, which could recognize any movement of user's wrist (like paddling geometric graphics) and give machine-voice-guide as man-machine feedback, is desired. In this paper, by using acceleration integral calculation to infer the spatial relative displacement and Kalman filter technology to reduce null-drift effect, user wrist's any exact MIP and continuous movement trajectory could be detected well. The testing results show that such a technique is valid in reflecting various spatial movements accurately and fast, which provides solid basis for realizing movement control and make it available in any wearable sensor application.

Key-Words: - CVD; SPG; MIP; pattern recognition; spatial tracking; MIMU

1 Introduction

Cardiovascular disease (CVD) involves the diseases of heart and/or blood vessels (arteries, capillaries and veins). It is the leading cause of death worldwide [1]. E-home healthcare aims at the daily health monitoring and the prevention of occurring CVD suddenly. Electrocardiogram (ECG) and echocardiography signals are not convenient for home usage; instead sphygmogram (SPG) as a signal noninvasively and easily obtained from the radial artery of wrist can reflect the physiological and pathological changes of heart and blood circulation system. Consequently, a mobile e-home healthcare system using pulse sensor to collect SPG signal, giving real-time intelligent analysis for CVD prognosis is researched and developed by our research group.

Specifically, the system uses the piezoelectric film pulse sensor to detect SPG signal by wearing it on user's wrist firmly and stably. Based on SPG morphological feature, hemodynamic parameters can be derived and served as input of intelligent analysis to conclude status of cardiovascular health and work out healthcare suggestions [2]. To comply with the pervasive monitoring trend, the front-end SPG acquisition sub-system is designed as wearable device enabling user collect his/her own physiological data at long time period in a comfortable way. However, practically the acquisition procedure will be negatively affected by this humanized factor due to that user usually moves or takes incorrect posture without being aware of having worn the device and currently under signal sampling. Hence one of challenges for such novel scheme lies in solving difficulty and inefficiency of SPG sampling which otherwise extremely impairs the maneuverability of this pervasive monitoring.

To tackle such a formidable problem caused by the absence of recognizing user's movement or incorrect posture (MIP) and lack of man-machine feedback to adjust SPG sampling procedure in real-time, an interactive MIP-awareness SPG sampling technique through using micro inertial measurement unit (MIMU) and pattern recognition is proposed [3]. In that solution, 24 kinds of MIP have been successfully recognized. But for real wearable application in which user's MIP emerges diversity and randomness, this recognition scheme based on limited MIP database is far less from meeting the requirement in detecting exact MIP and responding to user the definite prompt for adjusting such MIP.

Therefore, an innovative wearable SPG sampling technique through spatial movement tracking is proposed in this paper. By employing this technique fundamentally the unpredicted MIP can be explicitly recognized then the machine-voice prompt function is triggered thus to inform and guide the user to

eliminate his/her artificial disturbance efficiently. In next section the proposed technique will be depicted, followed by elaborating the spatial movement tracking. After the illustration of test results the conclusion will be given finally.

2 System Overview

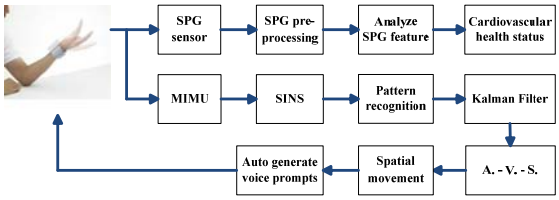

Fig. 1. Function diagram of SPG sampling technique through using pattern recognition and spatial tracking based on MIMU (A., V. and S. denotes acceleration, displacement and velocity individually, 'A. – V. – S.' reprensents displacement obtained by integral of velocity while the velocity obtained by integral of acceleration)

Fig. 1 demonstrates the working process of purposed system, in which MIMU is mounted with the SPG sensor wearing on user's wrist. MIMU detects the change of attitude information in 3 dimensions individually caused by various movements of user's wrist. Therein, the acceleration signal output by accelerometer is utilized for displacement calculation. The strapdown inertial navigation system (SINS) is responsible for computing attitude angle values which are used as parameters to estimate the motion type in later pattern recognition part. The Kalman filter is adopted to eliminate the error of acceleration signal. After reconstruction of velocity and displacement the specific spatial movement can be tracked. Correspondently the relevant voice prompts for guiding user's MIP are generated automatically in real-time way.

3 Pattern Recognition

3.1 SINS

An inertial navigation system (INS) is a navigation aid that uses a computer, accelerometers and gyroscopes to calculate the position, orientation and velocity of a moving object continuously without external references. SINS is INS with sensors strapped to the vehicle that is the SPG sensor in this proposed system. The SINS might be sub-divided further into the following component parts: inertial instrument block; instrument support electronics; coordinate transform; navigation computation; carrier's attitude information, which are shown in Fig. 3 [6].

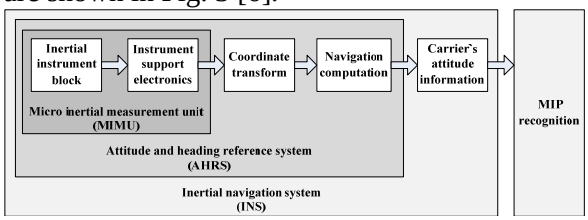

Fig. 2. Components and function diagram of SINS

Concretely, the adapted and implemented MIMU module here integrates GY-29-ADXL345 accelerometer, L3G4200D gyroscope and LSM303DLH compasses together (Fig. 3 (a)); the coordinate transform converts the fixed geographic coordinate system (x_p , y_p , z_p) to the moving carrier's coordinate system (x_p , y_p , z_p). It is supposed that the carrier's coordinate system rotates the angle (θ , γ , ψ) to geographic coordinate system. Then a transition matrix $\mathbf{C}_p^b$ is obtained as (1):

$$\mathbf{C}_p^b = \begin{bmatrix} \cos\gamma & 0 & -\sin\gamma \\ 0 & 1 & 0 \\ \sin\gamma & 0 & \cos\gamma \end{bmatrix} \begin{bmatrix} 1 & 0 & 0 \\ 0 & \cos\theta & \sin\theta \\ 0 & -\sin\theta & \cos\theta \end{bmatrix} \begin{bmatrix} \cos\psi & -\sin\psi & 0 \\ \sin\psi & \cos\psi & 0 \\ 0 & 0 & 1 \end{bmatrix} \quad (1)$$
$$= \begin{bmatrix} \cos\gamma\cos\psi + \sin\gamma\sin\theta\sin\psi & -\cos\gamma\sin\psi + \sin\gamma\sin\theta\cos\psi & -\sin\gamma\cos\theta \\ \cos\theta\sin\psi & \cos\theta\cos\psi & \sin\theta \\ \sin\gamma\cos\psi - \cos\gamma\sin\theta\sin\psi & -\sin\gamma\sin\psi - \cos\gamma\sin\theta\cos\psi & \cos\gamma\cos\theta \end{bmatrix}$$

Here, the coordinate system always maintains as rectangular coordinate system during the rotation. So $\mathbf{C}_p^b$ is an orthogonal matrix and has feature as shown in (2):

$$\left(\mathbf{C}_p^b\right)^{-1} = \mathbf{C}_b^p = \left(\mathbf{C}_p^b\right)^T \quad (2)$$

After navigation computation by solving Eq. (2), the carrier's attitude information is derived as three attitude angles relative to the local horizontal plane: roll, pitch and yaw (θ , γ , ψ) [7].

Fig. 3. (a) The adapted and implemented circuit of MIMU; (b) Operation of MIMU-mounted SPG sampling

3.2 MIP Database and Recognition

In [3], 32 kinds of MIP are summed up. But only 24 MIP occurring at left forearm where the MIMU located is successful recognized, which can be

classified into three groups: movement, incorrect posture and incorrect posture with movement as listed on Table 1.

An accuracy given here describes the MIP recognition result in a test [3]. The test asking 5 volunteers to randomly make any movement or set themselves in incorrect posture, which should be in scope of 24 kinds of MIP in the database. The result shows most left forearm movement can be recognized successfully, and the accuracy is good enough in practical sampling.

TABLE I. MIP DATABASE AND TEST RESULT

No.	Groups	Category of movement or incorrect posture		Abbreviation	Accuracy (%)
1	M	Parallel to the ground	Forward-backward	LFP-FB	80
2			up-down	LFP-UD	96
3			left-right	LFP-LR	92
4			wrist-twist	LFP-WT	100
5	IP	Lay naturally to the ground		LFP	100
6		lay down 45 degree to the ground		LFL45	96
7		up-lift 45 degree to the ground		LFU45	96
8		up-lift vertical to the ground		LFU	100
9	MIP	Lay naturally to the ground	Forward-backward	LFL-FB	92
10			up-down	LFL-UD	100
11			left-right	LFL-LR	96
12			wrist-twist	LFL-WT	100
13		lay down 45 degree to the ground	Forward-backward	LFL45-FB	88
14			up-down	LFL45-UD	100
15			left-right	LFL45-LR	96
16			wrist-twist	LFL45-WT	100
17		up-lift 45 degree to the ground	Forward-backward	LFU45-FB	88
18			up-down	LFU45-UD	100
19			left-right	LFU45-LR	96
20			wrist-twist	LFU45-WT	100
21		up-lift vertical to the ground	Forward-backward	LFU-FB	92
22			up-down	LFU-UD	100
23			left-right	LFU-LR	96
24			wrist-twist	LFU-WT	100

4 Spatial Movement Tracking

4.1 Kalman Filter

Based on previous researches, accelerometer has been proved having various errors. The main errors can be divided into two types: inertial sensor errors and computation error. The inertial sensor errors include scale factor error, zero drift error and random error [4].

To reduce the noise coming from the accelerometer and inhibit inertial sensor errors, the improved Kalman filter [5] [6] by adding a new acceleration state is adapted to MIMU. In this filter, the measurement model based on statistical nature of the system is used to estimate the acceleration data and forecast the future state of system. Using a weight function called Kalman gain; a minimum error variance has been obtained [7].
Suppose that the Kalman filter model is:

$$\mathbf{x}_{k+1} = \boldsymbol{\varphi}_k \mathbf{x}_k + \boldsymbol{\omega}_k \tag{3}$$

where vector $\mathbf{x}_k$ denotes system state (considering that there are 3-axis and each has displacement and velocity, thus $\mathbf{x}_k = \left[s_x,\ s_y,\ s_z,\ v_x,\ v_y,\ v_z \right]^T$); $\boldsymbol{\omega}_k$ denotes noise vector with its covariance $\mathbf{Q}_k$; $\boldsymbol{\varphi}_k$ is a 6×6 transition matrix at time t_k. Here assume that the position will be measured every Δt_k seconds. Then transition matrix can be set as:

$$\boldsymbol{\varphi}_k = \begin{bmatrix} 1 & 0 & 0 & \Delta t_k & 0 & 0 \\ 0 & 1 & 0 & 0 & \Delta t_k & 0 \\ 0 & 0 & 1 & 0 & 0 & \Delta t_k \\ 0 & 0 & 0 & 1 & 0 & 0 \\ 0 & 0 & 0 & 0 & 1 & 0 \\ 0 & 0 & 0 & 0 & 0 & 1 \end{bmatrix} \tag{4}$$

According to [9] the observation of 3-axis displacement $\mathbf{z}_k$ of state $\mathbf{x}_k$ at time t_k can be obtained as:

$$\mathbf{z}_k = \mathbf{H}\mathbf{x}_k + \mathbf{v}_k \tag{5}$$

where $\mathbf{v}_k$ is the measurement noise with its covariance $\mathbf{P}_k$; $\mathbf{H}$ is the measurement matrix and can be set initially as:

$$\mathbf{H} = \begin{bmatrix} 1 & 0 & 0 & 0 & 0 & 0 \\ 0 & 1 & 0 & 0 & 0 & 0 \\ 0 & 0 & 1 & 0 & 0 & 0 \end{bmatrix} \tag{6}$$

Because $\boldsymbol{\omega}_k$ and $\mathbf{v}_k$ are zero mean, so their white Gaussian noise covariances are calculated by (7) respectively.

$$\begin{aligned}\mathbf{Q}_k &= E\left[\boldsymbol{\omega}_k \quad \boldsymbol{\omega}_k^T\right] \\ \mathbf{P}_k &= E\left[\mathbf{v}_k \quad \mathbf{v}_k^T\right]\end{aligned} \tag{7}$$

where E means expected value operator.

Based on this, the estimated state and the predicted state of Kalman filter are shown as follows:

$$\begin{aligned}\hat{\mathbf{x}}_k(+) &= \hat{\mathbf{x}}_k(-) + \overline{K}[\mathbf{z}_k - \mathbf{H}\hat{\mathbf{x}}_k(-)] \\ \hat{\mathbf{x}}_{k+1}(-) &= \boldsymbol{\varphi}_k \hat{\mathbf{x}}_k(+)\end{aligned} \tag{8}$$

where $\overline{K}$ denotes Kalman gain. '$(-)$' indicates prior values of variables (before information in the measurement is used); '$(+)$' indicates posterior values of variables (after information in the measurement is used).

Then add the acceleration state to such filter, thus the Kalman model becomes:

$$\hat{\mathbf{x}}_k(+) = \hat{\mathbf{x}}_k(-) + \overline{K}[\mathbf{z}_k - \mathbf{H}\hat{\mathbf{x}}_k(-)] + \mathbf{B}_k\mathbf{U}_k \tag{9}$$

where $\mathbf{U}_k = [a_x, a_y, a_z]^T$ is the added state, a represents acceleration via each axis; $\mathbf{B}_k$ is shown as follows:

$$\mathbf{B}_k = \begin{bmatrix} \frac{\Delta t_k^2}{2} & 0 & 0 \\ 0 & \frac{\Delta t_k^2}{2} & 0 \\ 0 & 0 & \frac{\Delta t_k^2}{2} \\ \Delta t_k & 0 & 0 \\ 0 & \Delta t_k & 0 \\ 0 & 0 & \Delta t_k \end{bmatrix} \tag{10}$$

4.2 Acceleration integral calculation

Founded on physical principal, displacement can be obtained by double integral of acceleration. So via continuously detecting target's 3-axis real-time acceleration and doing integral operation with those acceleration data the target's instantaneous velocity and accumulative space trajectory can be calculated. Suppose the SPG sampling starts from the time t_0, then the corresponding velocity and displacement until time t are derived as (11).

$$\begin{aligned}v(t) &= \int_{t_0}^{t} a(t)dt + v(t_0) \\ s(t) &= \int_{t_0}^{t} v(t)dt + s(t_0)\end{aligned} \tag{11}$$

Owing to the MIMU output is a series of discrete data, (11) can be represented as (12) in which $\mathbf{s}(t_0) = 0$, $n = 1, 2, \ldots N$.

$$\begin{aligned}\mathbf{v}[n] &= \sum_{k=1}^{n} \frac{\mathbf{a}[k] + \mathbf{a}[k-1]}{2}\Delta t \\ \mathbf{s}[n] &= \sum_{k=1}^{n} \frac{\mathbf{v}[k] + \mathbf{v}[k-1]}{2}\Delta t\end{aligned} \tag{12}$$

To simplify the calculation, iteration is adapted on (12), thus to get (13) as follows:

$$\begin{aligned}\mathbf{v}[n] &= \mathbf{v}[n-1] + \frac{\mathbf{a}[n] + \mathbf{a}[n-1]}{2}\Delta t \\ \mathbf{s}[n] &= \mathbf{s}[n-1] + \frac{\mathbf{v}[n] + \mathbf{v}[n-1]}{2}\Delta t\end{aligned} \tag{13}$$

Thereby, the current instantaneous velocity and displacement can be obtained by utilizing last calculation output of $\mathbf{v}[n]$ and $\mathbf{s}[n]$. Accordingly, the target's x-, y-, z-axis instantaneous velocity is derived individually from the acceleration output of 3-axis MIMU as (14) shows:

$$\begin{aligned}\bar{\mathbf{v}}_x[t] &= \bar{\mathbf{v}}_x[t-\Delta t] + \frac{\bar{\mathbf{a}}_x[t] + \bar{\mathbf{a}}_x[t-\Delta t]}{2}\Delta t \\ \bar{\mathbf{v}}_y[t] &= \bar{\mathbf{v}}_y[t-\Delta t] + \frac{\bar{\mathbf{a}}_y[t] + \bar{\mathbf{a}}_y[t-\Delta t]}{2}\Delta t \\ \bar{\mathbf{v}}_z[t] &= \bar{\mathbf{v}}_z[t-\Delta t] + \frac{\bar{\mathbf{a}}_z[t] + \bar{\mathbf{a}}_z[t-\Delta t]}{2}\Delta t\end{aligned} \tag{14}$$

As the same argument, target's 3-axis displacement at time t is calculated separately as follows:

$$\begin{aligned}\mathbf{s}_x[t] &= \mathbf{s}_x[t-\Delta t] + \frac{\bar{\mathbf{v}}_x[t] + \bar{\mathbf{v}}_x[t-\Delta t]}{2}\Delta t \\ \mathbf{s}_y[t] &= \mathbf{s}_y[t-\Delta t] + \frac{\bar{\mathbf{v}}_y[t] + \bar{\mathbf{v}}_y[t-\Delta t]}{2}\Delta t \\ \mathbf{s}_z[t] &= \mathbf{s}_z[t-\Delta t] + \frac{\bar{\mathbf{v}}_z[t] + \bar{\mathbf{v}}_z[t-\Delta t]}{2}\Delta t\end{aligned} \tag{15}$$

In time period $t - \Delta t$, the target's spatial movement displacement is defined as:

$$\mathbf{s}_{\Delta}[t]=\sqrt{(\mathbf{s}_X[t]-\mathbf{s}_X[t-\Delta t])^2+(\mathbf{s}_Y[t]-\mathbf{s}_Y[t-\Delta t])^2+(\mathbf{s}_Z[t]-\mathbf{s}_Z[t-\Delta t])^2} \quad (16)$$

So at the time *t*, target's spatial coordinate is ($\mathbf{S}_x[t]$, $\mathbf{S}_y[t]$, $\mathbf{S}_z[t]$). Thus the corresponding movement trajectory can be obtained.

5 Test Result

In order to validate the effectiveness of proposed technique, the following tests are conducted. The first test indicates the performance of Kalman filter. Fig. 4(a) is the comparison result of *x*-axis acceleration output with static wrist while Fig. 4(b) shows the comparison result with moving wrist. Obviously the signals are smoother and have less mutation after adding Kalman filter's processing.

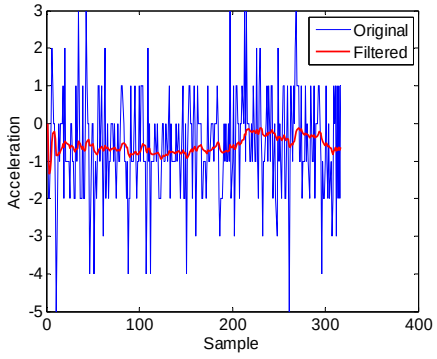

(a)

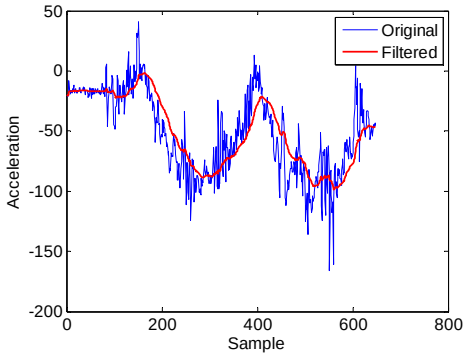

(b)

Fig. 4. (a) *x*-axis acceleration static output; (b) *x*-axis acceleration output by wrist moving

Furthermore, to evaluate the whole spatial movement tracking technique, an experiment is conducted by asking 1 volunteer to test various MIP randomly wearing the MIMU-mounted piezoelectric film SPG sensor on his wrist (Fig. 3 (b)). Fig. 5 demonstrates two typical examples of spatial movement tracking result. The volunteer paddles a rectangle spatially and the corresponding trajectory result is revealed in Fig. 5 (a); and the other time he paddles a triangle whose tracking result is shown in Fig. 5 (b).

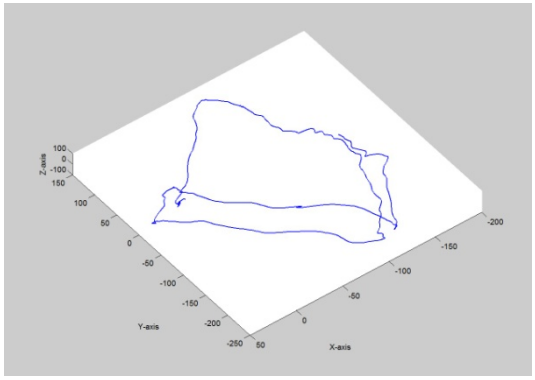

(a)

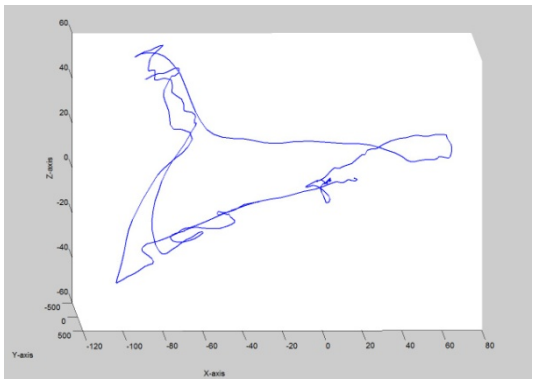

(b)

Fig. 5. (a) The rectangle spatial tracking result; (b) The triangle spatial tracking result

Although the shapes shown in Fig. 5 do not strictly meet the formal definition of rectangle and triangle because of the fact that unlike using pen to drew on paper the shape drew spatially usually has greater deviation, the tracking can still be recognized correctly through recognizing its several key characteristics. In short, the spatial movement tracking shows effectiveness in recognizing various MIP to a certain extent.

As to the future perfection of this technique, the following aspects can be improved. Firstly, some compensation algorithm is expected to eliminate the effect of wrist's trembling. Moreover, in practical test, the start and end points of each movement tracking curve are not in ideal condition so it has potential of getting more accurate trajectory modeling by removing the influence of previous velocity and displacement result.

6 Conclusion

An innovative technique for fast sampling qualified SPG signal by using pattern recognition and acceleration integral calculation to infer the spatial relative displacement and Kalman filter technology to reduce null-drift effect is proposed and implemented. It integrates MIMU hardware platform and use MIP pattern database to quickly recognize first. Then used spatial movement tracking method to detect wrist's motion to recognize any other MIP without provide database. At the end automatically thus trigger machine-voice-guide as man-machine feedback to eliminates user's disturbance with high efficiency. The computation of spatial movement pattern by utilizing acceleration output signal taking from MIMU is well illustrated. About three fifth extended sampling time caused by user's MIP has been decreased. The global performance of the proposed technique is outstanding. Hence, this spatial movement tracking technique is proved to be effective in fast sampling qualified SPG signal and has potential usage in other wearable sensor applications.

Acknowledgement

This work is supported by Research Committee of University of Macau under grant No. MYRG184(Y2-L3)-FST11-DMC and also by the Science and Technology Development Fund (FDCT) of Macau S.A.R with project ref. No. 018/2009/A1.

References:

[1] W. H. Organization. Global atlas on cardiovascular disease prevention and control. http://www.who.int/cardiovascular_diseases/en/

[2] B.N.Li, B.B. Fu & M.C.Dong, "Development of a mobile pulse waveform analyzer for cardiovascular healthmonitoring" *Computers in Biology and Medicine*, 38(4) 438-445, Apr 2008, Elsevier.

[3] GAN Zhen, FU BinBin, ZHENG XiaLi, DONG MingChui, "Interactive MIP-awareness SPG Sampling Technique", 6th WSEAS International Conference on Biomedical Electronics and Biomedical Informatics (BEBI13), Baltimore, MD, USA, Sep. 17-19, 2013

[4] Gao, J., Webb, P., Gindy, N., "Error reduction for an inertial-sensor-based dynamic parallel kinematic machine positioning system", Measurement Science and Technology, v 14, n 5, May, 2003, p 543-550.

[5] Pang, Grantham, Liu, Hugh, "Evaluation of a low-cost MEMS accelerometer for distance measurement", Theory and Applications, v 30, n 3, Mar, 2001, p 249-265.

[6] Dripps, J.H. "Introduction to model based digital signal processing", IEE Colloquium (Digest), n 009, 1997, p 1/1-1/4.

[7] Kaplan, E.D., Lewis, S., "Understanding GPS:", Principles and Applications Journal of Electronic Defense, v 20, n 1/SUP, 1997, p 81.

[8] [8] Trujillo, D.M., Carter,A.L., "NEW APPROACH TO THE INTEGRATION OF ACCELEROMETER DATA", Earthquake Engineering & Structural Dynamics, v 10, n 4, Jul-Aug, 1982, p 529-535.

[9] [9] Wikipedia. Kalman filter. http://en.wikipedia.org/wiki/Kalman_filter